Article:
Wang, H, Jia, Y, Shi, M et al. (2 more authors) (2023) A Mutually Beneficial Operation Framework for Virtual Power Plants and Electric Vehicle Charging Stations. IEEE Transactions on Smart Grid. ISSN 1949-3053

https://doi.org/10.1109/TSG.2023.3273856

A Mutually Beneficial Operation Framework for Virtual Power Plants and Electric Vehicle Charging Stations

Han Wang, *Graduate Student Member, IEEE,* Youwei Jia, *Member, IEEE,* Mengge Shi, *Graduate Student Member, IEEE,* Chun Sing Lai, *Senior Member, IEEE,* Kang Li, *Senior Member, IEEE*

***Abstract*-Virtual power plants (VPPs) and electric vehicle (EV) charging stations (CSs) have been attracting much attention in recent years. However, existing research rarely concerns the cooperation between VPPs and CSs that are managed by different stakeholders. To facilitate the cooperation between VPPs and CSs, this work proposes a cooperative operation framework for a multi-stakeholder VPP-CSs system. In the proposed cooperative framework, day-ahead offering and real-time balancing models are developed to maximize the total benefit of the VPP-CSs system. To support a more flexible operation of the VPP-CSs system with EV energy flexibility, an EV user incentive program is proposed for acquiring EV battery access rights. The conflicting interests of different stakeholders are addressed by a τ-value cost allocation method. To alleviate the computational burden in calculating the τ-values, a maximum right cost estimation approach is proposed. Case studies confirm that the proposed methods can provide superior performance by increasing 4.6% of VPP profit, increasing 20.7% of CS profit, reducing 16.3% of EV user charging fees, and achieving 99.2% of τ-value estimation accuracy.**

***Index Terms*-virtual power plant, charging stations, incentives, multi-stakeholder, τ-value estimation**

I. INTRODUCTION

The growing concerns about climate change are boosting the worldwide decarbonization trend [1]. To achieve cleaner production and more efficient energy utilization, virtual power plant (VPP) [2] and electric vehicle (EV) [3] researches have attracted much attention in recent years.

To further unleash the potential of VPPs and EVs in supporting sustainable developments, researchers have made pioneering efforts in integrating EV energy scheduling into the VPP operation [4]. In the literature, EVs are normally used as energy storage that can be directly managed by the VPP operator to strengthen the VPP performance. For example, To enhance the VPP power quality, the energy flexibility of EVs is controlled by the VPP to smooth out the energy fluctuations of renewable generators in [5] and [6]. Besides, to improve the VPP profitability, the VPP operator can utilize the EV energy flexibility to compensate for energy deviations stemming from various uncertain factors, such as in [7]–[12].

Existing research has made remarkable progress in integrating EVs into the VPP operation. However, most proposals assume the same ownership for both the VPP and EV charging facilities and little has been done on addressing the challenges when they are owned by different stakeholders. In real-world applications, public charging stations (CSs) are the major EV charging facility owners [13]. CSs can also act as natural aggregators for EV energy scheduling because they can deal with a greater number of charging piles than individual household charger owners. Hence, some early attempts have been made to incorporate CSs into the VPP operation.

In [14], a VPP comprising dwellings, renewables, energy storage systems, and a CS is investigated. However, the VPP considered in [14] owns the CS and gives direct dispatching signals to control the CS operation. In [15], a VPP composed of renewables and a CS is considered. The work in [15] also assumes that the VPP and CS have the same interest and there is a central control unit to coordinate the CS operation with other VPP components. In [16], the authors considered a VPP with thermal generators, renewables, and energy storage. A self-interested CS is also considered in [16], and the interactions between the VPP and CS are modeled by using a Stackelberg game framework. In [17], a VPP containing distributed generation and a self-interested CS is investigated. The CS operation in [17] is affected by the VPP price signals. Hence, the VPP in [17] can set different prices to indirectly adjust the charging load of the CS in [17]. Though [16], [17] considered VPP and CSs with different ownerships, the CSs in [16], [17] can only passively respond to VPP price signals instead of proactively interacting with the VPP operator, which can weaken the functionality of EVs as energy buffers. To address this issue and allow proactive interactions between the VPP and CSs, this work proposes a mutually beneficial operation framework for VPP-CSs systems consisting of a distributed generator-based VPP and multiple CSs.

The proposed mutually beneficial VPP-CSs operation framework includes day-ahead offering and real-time balancing models. In the day-ahead stage, CSs schedule their energy procurements to satisfy the expected EV charging demand under both the EV charging demand and market price

This work was supported in part by the National Natural Science Foundation of China (72071100), Shenzhen Basic Research Program (JCYJ20210324104410030), and Young Elite Scientist Sponsorship Program by CSEE (CSEE-YESS-2020027).

Han Wang is with the Department of Electrical and Electronic Engineering and the University Key Laboratory of Advanced Wireless Communication of Guangdong Province, Southern University of Science and Technology, Shenzhen, 518055, China. and also with the School of Electronic and Electrical Engineering, University of Leeds, Leeds, LS2 9JT, U.K. (e-mail: elhwa@leeds.ac.uk)

Youwei Jia is with the Department of Electrical and Electronic Engineering and the University Key Laboratory of Advanced Wireless Communication of Guangdong Province, Southern University of Science and Technology, Shenzhen, 518055, China. (e-mail: jiayw@sustech.edu.cn)

Mengge Shi is with the Department of Electrical and Electronic Engineering and the University Key Laboratory of Advanced Wireless Communication of Guangdong Province, Southern University of Science and Technology, Shenzhen, 518055, China. (e-mail: shimg2019@mail.sustech.edu.cn)

C. S. Lai is with the Brunel Interdisciplinary Power Systems Research Centre, Department of Electronic and Electrical Engineering, Brunel University London, London, UB8 3PH, U.K. (e-mail: chunsing.lai@brunel.ac.uk).

K. Li is with the School of Electronic and Electrical Engineering, University of Leeds, Leeds, LS2 9JT, U.K. (e-mail: k.li1@leeds.ac.uk).

uncertainties. After CSs complete their energy scheduling, the VPP collects CS energy procurement plans to generate the aggregated day-ahead energy market offering strategy considering the price and renewable uncertainties. In the real-time stage, the VPP and CSs coordinately schedule the generator generations and EV charging plans to compensate for energy deviations stemming from forecast errors.

The day-ahead offering and real-time balancing models in the proposed operation framework are meant to maximize the total benefit of the VPP-CSs system. To maximize the total benefit of the VPP-CSs system, EV energy flexibility is a crucial solution to mitigate the negative impacts of forecast errors. A key enabler of utilizing EV energy flexibility is EV user cooperation, which directly affects the regulation capability of CSs. When no incentives are provided to change the charging behaviors, EV users tend to recharge their EVs as quickly as possible to mitigate range anxieties [18], leaving no EV energy flexibility for the VPP-CSs system. Hence, the problem of how to encourage EV users to respond to control signals from CSs awaits to be addressed.

Previous incentivizing methods can be roughly classified as static and dynamic methods. The static incentive programs have low incentive signal update frequency. That is, the incentive signals will remain effective for a relatively long time in static programs. Typical static incentive programs for EV users include time-of-use pricing and critical peak pricing. In [19]–[21], the time-of-use pricing program is used to shift the EV charging load from high-price periods to low-price periods. In [22], [23], the time-of-use and critical peak pricing programs are jointly applied to affect EV user charging behavior. As compared to static incentive programs, dynamic incentive programs update incentive signals more frequently to handle short-term system variations. Typical dynamic incentive programs include transactive control and dynamic pricing methods. In [24]–[26], the transactive control method is applied to manage EV charging load through local transactive markets. In [27]–[29], the real-time dynamic pricing strategy is applied to instantly affect the EV charging load to maximize the CS profit or reduce residential load peaks.

As a hybrid method that combines the advantages of both static and dynamic methods, the incentive method proposed in [30] is proven effective in encouraging EV user cooperation. However, two factors can restrict the efficiency of the methods proposed in [30]. Firstly, the vehicle-to-grid (V2G) operation is not considered. Also, the uniform pricing strategy in [30] can discourage EV energy flexibility utilization on some occasions. Hence, on top of the methods proposed in [30], an enhanced incentive program is proposed in this work to further encourage EV user cooperation.

After maximizing the total benefit of the VPP-CSs system by using both generator and EV energy flexibility, the conflicting interests between different stakeholders in the system need to be addressed to maintain the willingness of different stakeholders to cooperate. In power engineering, the Shapley Value method is the most popular approach for handling the cost allocation problem in cooperative games [31]–[33]. However, the application of the Shapley Value method is hindered by its computational intractability, which makes it impractical for the considered cost allocation problem. To solve the cost allocation problem while keeping the computational burden under control, an estimated τ-value cost allocation method is proposed in this work. In the conventional τ-value method, all possible sub-coalitions need to be evaluated to compute the τ-values, which is bluntly unrealistic for the considered cost allocation problem. By utilizing some key features in the τ-value calculation process, the proposed estimated τ-value method can significantly reduce the number of evaluated sub-coalitions, meanwhile, achieving a high estimation accuracy.

To summarize, this work is dedicated to proposing a cooperative operation framework for VPPs and CSs with different ownerships. To handle the interest conflicts between different stakeholders, an EV user incentive program and a cost allocation method are proposed in this paper. To this end, the original contributions of this work can be summarized as follow:

- A multi-stakeholder VPP-CSs system consisting of a distributed generator-based VPP and multiple CSs is investigated. A cooperative operation framework is proposed to handle the interactive day-ahead offering and real-time balancing problems of the VPP-CSs system.
- An EV user incentive program is proposed. Compared to the methods in [30], the proposed incentive program can achieve more EV user cost reduction, higher EV energy flexibility utilization, and lower total system cost.
- An estimated τ-value cost allocation method is proposed to efficiently address the cost allocation problem of the VPP-CSs system.

The remainder of this paper is organized as follows: Section II presents the proposed VPP-CSs operation framework and the EV user incentive program. Section III gives the detailed problem formulations of the day-ahead offering and real-time dispatching models. Section IV provides the estimated τ-value cost allocation method. Numerical results are given and discussed in Section V. Section VI concludes this work.

II. MODEL DESCRIPTION

This section first presents an overview of the investigated VPP-CSs system, then provides the details of the proposed EV user incentive program.

A. VPP-CSs System

The configuration of the considered VPP-CSs system is displayed in Fig. 1.

This work considers a distributed generator-based VPP (with both wind and thermal power plants) and multiple CSs (with level 2 charging rate) to form a VPP-CSs system. Due to the heavy capital cost of energy storage devices [34], only renewable generators and thermal power plants are considered to form the VPP, and energy storage devices are not included in the VPP configuration. In this system, the stakeholders include the VPP, the CSs, and EV users. The VPP can directly manage the wind and thermal power plants to participate in electricity markets. The CSs can directly manage the charging/discharging behavior of EVs. In this configuration, the CSs can also indirectly benefit from the competitive market price through the VPP. The VPP benefits from CSs by indirectly making use of the energy flexibility of EVs. Due to the small capacities of individual EVs, EV users are not involved in the market operation. To address the interests of EV users, the contribution of EV users is financially remunerated through an incentive program.

The proposed operation framework for the VPP-CSs system is summarized in Fig. 2. The considered VPP-CSs system participates in both the day-ahead energy market and the balancing market. Under this framework, the considered VPP-CSs system needs to face uncertainties in market price, renewable generation, and EV charging demand.

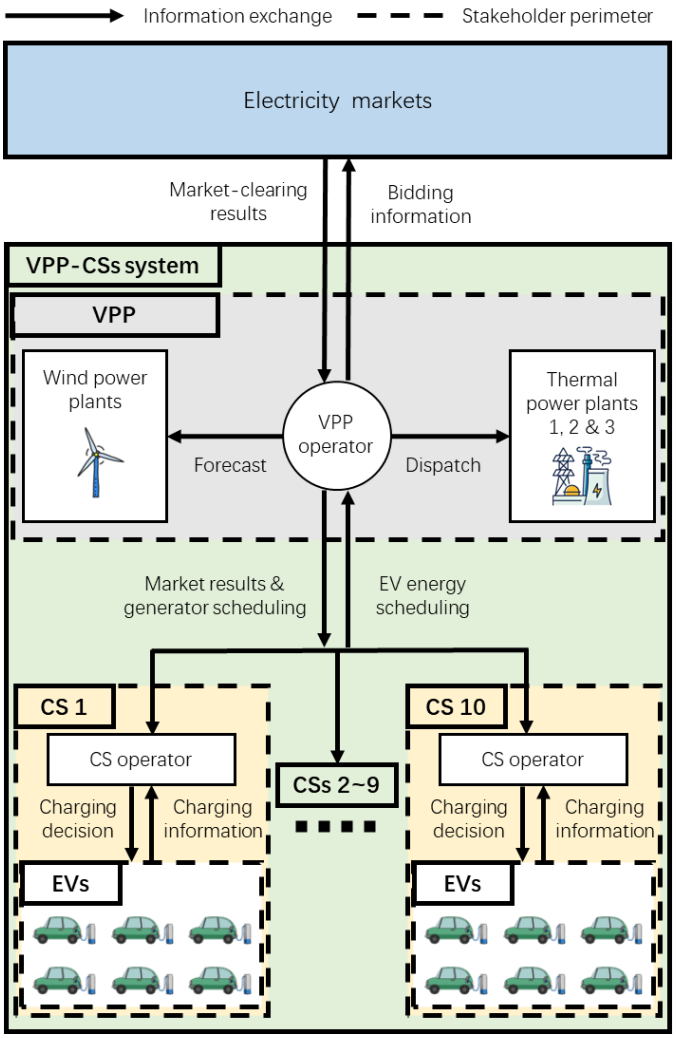

Fig. 1. Configuration of the VPP-CSs system.

In the day-ahead market, the investigated VPP-CSs system acts as a price-taker who submits offering curves to the market operator. The submitted offering curves should contain price-quantity pairs that reflect how much energy the VPP-CSs system is willing to sell to or buy from the day-ahead market at different market-clearing prices. In the balancing market, due to uncertainties in renewable generation and EV charging demand, the VPP-CSs system is considered a deviator. The balancing market settles the energy deviations of the considered VPP-CSs system by using penalty prices. Specifically, energy surplus will be sold at a lower price, and energy deficiency needs to be bought at a higher price [35]:

$$\lambda_t^{D+} = \omega^+ \lambda_t^{DA} \quad (1)$$

$$\lambda_t^{D-} = \omega^- \lambda_t^{DA} \quad (2)$$

$$\omega^+ \geq 1 \quad (3)$$

$$\omega^- \leq 1 \quad (4)$$

where λ_t^{DA} is the day-ahead energy market-clearing price at time t; The balancing prices for energy deficiency and energy surplus are given by λ_t^{D+} and λ_t^{D-}, respectively. Parameters φ^+ and φ^- are the market penalty coefficients, which can reflect how severely the market penalizes energy deviations.

In the day-ahead stage, CSs need to forecast the market price and charging demand. Based on the forecast information, CSs can schedule their energy procurement plans under both market price and EV charging demand uncertainties to minimize their energy procurement cost. After CSs complete their energy procurement plans, the VPP collects the CS energy procurement plans to develop the aggregated VPP-CSs system offering curves under uncertain price and renewable power generation. Before developing the aggregated offering curve, the VPP needs to predict the market price and renewable energy production. With the forecast information and CS energy plans, the VPP can schedule the thermal power plants and offer different energy quantities at different price scenarios to maximize its profit. Once the market is cleared, the VPP gets paid by the market for energy sales or pays the market for energy procurements at the market-clearing price. Besides, the CSs should also pay the VPP for their scheduled energy procurements or get paid for energy sales at the market-clearing price.

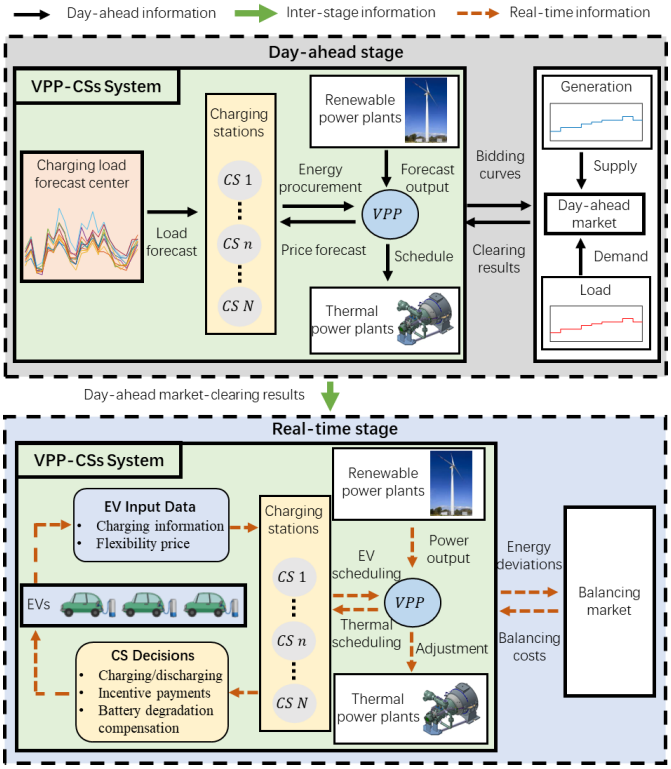

Fig. 2. Operation framework of the considered VPP-CSs system.

To handle uncertainties in the day-ahead stage, uncertainties in renewable productions and EV charging demands are modeled using intervals. Each interval is characterized by a forecast value (i.e., fv_t^r for renewable production and fv_t^{cs} for CS charging demand) and an uncertainty coefficient that indicates the accuracy of the forecasts (i.e., σ^r for renewable production and σ^{cs} for CS charging demand), as shown below:

$$(1-\sigma^r) fv_t^r \leq u_t^r \leq \min\{(1+\sigma^r) fv_t^r, P_{cap}^r\} \quad (5)$$

$$(1-\sigma^{cs}) fv_t^{cs} \leq u_t^{cs} \leq \min\{(1+\sigma^{cs}) fv_t^{cs}, P_{cap}^{cs}\} \quad (6)$$

where u_t^r and u_t^{cs} represent the renewable power production and EV charging demand, respectively. The installed renewable power generation capacity is given by P_{cap}^r, and the CS charging capacity is given by P_{cap}^{cs}.

Besides, the market price uncertainty is modeled using representative scenarios. The representative price scenarios are selected to cover price scenarios ordered from high to low in an unbiased manner [36]. To this end, the CS Day-ahead energy scheduling problems can be formulated as stochastic minimax regret problems, which minimize the expected worst-case regret under both EV charging demand and market price uncertainties. For the VPP, the day-ahead offering problems can be formulated as minimax regret optimization problems that minimize the worst-case regret regarding uncertain renewable power generation.

In the real-time stage, the VPP and CSs cooperatively schedule the thermal power plants and EV charging plans to minimize energy deviation costs resulting from the renewable output and EV charging demand forecast errors. In this stage, the market prices and EV charging information become known parameters, the remaining uncertain factor is renewable production. To handle the renewable uncertainty and keep up with the constantly updated EV charging information, a rolling horizon optimization approach is developed in this work. In the rolling horizon approach, the generator generation and EV charging decisions are continuously optimized to minimize the total operation cost. Notably, in this VPP-CSs system, the generator generation can be directly controlled, but the charging power of EVs cannot be arbitrarily changed since EVs belong to EV users instead of the VPP-CSs system. Hence, an EV user incentive program is proposed in the next subsection to remunerate EV users in exchange for EV charging power control rights.

B. EV User Incentives

By controlling the charging and discharging of batteries, EVs can play an important role in reshaping the aggregated load profile of the VPP-CSs system. However, controlling EV charging and discharging behaviors requires cooperation from EV users who wish to recharge their EVs as quickly as possible. Hence, a well-designed incentive program is of great significance to encourage EV user participation in smart charging and improve the overall profitability of the VPP-CSs system.

Existing incentive programs can be categorically classified as static and dynamic programs. Static incentive programs have the advantages of being simple and consistent, but dynamic programs can offer more controllability for CS operators to improve their profitability. By combining the strengths of both static and dynamic programs, the method proposed in [30] shows promising performances in encouraging EV energy flexibility utilization.

However, two factors can undermine the performance of the original methods proposed in [30]. Firstly, the V2G operation is not considered. The original method only utilizes the EV charging flexibility and ignores the discharging flexibility. As the V2G technology matures, the importance of utilizing EV discharging flexibility has been intensively researched [37]–[39]. Hence, the first improvement of the proposed incentive program is to encourage the V2G operation. Besides, the original method adopts the uniform pricing mechanism, which can discourage flexibility utilization on some occasions. By using the uniform pricing mechanism, the variation in EV users' willingness to respond to system regulation signals cannot be reflected, hence, reducing the efficiency of incentive programs in encouraging EV users. Compared to the uniform pricing mechanism, the pay-as-bid mechanism is more efficient in reflecting different EV users' willingness to offer their energy flexibility. Therefore, the second improvement in the proposed incentive program is to adopt the pay-as-bid mechanism to encourage more proactive EV users' participation. The proposed incentive program details are presented next.

In this work, EV users buy energy from CSs to recharge their EVs. Meanwhile, EV users can get paid by selling their EV energy flexibility to CSs. If the time-of-use pricing is applied to affect the charging behavior of EV users, EV users will need to wait for low-price hours to recharge their EVs if they wish to reduce their charging bills. Making EV users wait can disturb their parking and traveling plans, which causes inconvenience for EV users. Hence, the energy retail price at CSs for EV users to recharge their EVs is always the same. To encourage EV users to respond to regulation signals from CSs, incentives are used in the proposed incentive program to acquire EV battery access rights and control the charging process of EVs. In the proposed incentive program, the remuneration is based on the pay-as-bid and pay-as-use principles. That is, the payment for using the EV charging and discharging flexibility depends on both the EV user offering price γ_m (\$/kWh) and the quantity of adopted energy flexibility (kWh).

The adopted charging energy flexibility is the load shifted between different periods, and the adopted discharging energy flexibility is the energy injected back into the grid from EVs. Through the proposed incentive program, CSs will remunerate EV users for adopting their energy flexibility. Besides, battery degradation will also be compensated when discharging energy flexibility is adopted. The payment computations are schematically illustrated in Fig. 3, which shows how much will EV users be remunerated for adopting their energy flexibility. Fig. 3a shows the EV charging load before (left) and after (right) the scheduling. In hours 13 and 14, the CS not only reduces the EV charging power but also discharges the EV to inject power back into the grid. In hours 15 to 18, the EV charging power is increased to fulfill the EV charging demand. These EV power changes are summarized in Fig. 3b, in which one can observe that the EV user gets remunerated for both the reduced charging power (adopted charging energy flexibility) and the scheduled discharging power (adopted discharging energy flexibility).

Notably, increasing the EV charging load cannot generate remuneration for EV users. This is because EV users always tend to recharge their EVs as quickly as possible to reduce their range anxiety [18], and increasing the charging power can rarely cause inconvenience to EV users.

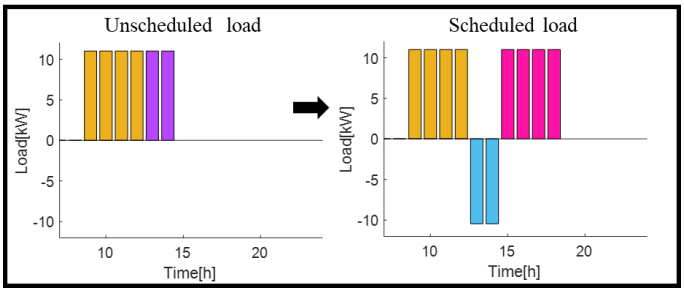

(a) Load scenarios.

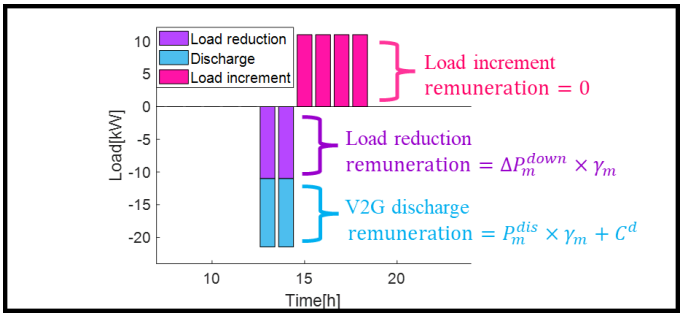

(b) Load change results.

Fig. 3. Payments for using EV energy flexibility.

When energy flexibility is adopted, the payment for EV user m is based on the adopted energy flexibility and the offering prices γ_m. To obtain the energy flexibility adopting results, the unscheduled charging load should be computed first. It is assumed that in the unscheduled charging scenario, EV users would recharge their EVs at the maximum charging power

immediately after they arrive at the CSs to mitigate their range anxieties. In the unscheduled charging scenario, the maximum charging power continues until EVs are fully charged. The charging load in the unscheduled charging scenario is defined as the unscheduled charging load $P_{m,t}^{us}$. In the unscheduled charging scenario, the unscheduled charging load $P_{m,t}^{us}$ of EV user m at time t can be summarized as follows:

$$P_{m,t}^{us} = \begin{cases} 0, & if\ SOC_{m,t-1} = SOC_m^{max} \\ \frac{SOC_m^{max} - SOC_{m,t}}{Cap_m}, & if\ P_m^{max} > \frac{SOC_m^{max} - SOC_{m,t-1}}{Cap_m \Delta t} \\ P_m^{max}, & if\ P_m^{max} \le \frac{SOC_m^{max} - SOC_{m,t-1}}{Cap_m \Delta t} \end{cases} \quad (7)$$

where SOC_m^{max} is the maximum state-of-charge (SOC) of EV m, P_m^{max} is the maximum charging rate of energy for EV m, and Cap_m is the battery capacity of EV m. The SOC of EV m at each scheduling period t is given by $SOC_{m,t}$, and Δt is the length of a scheduling time interval.

By using Eq (7), the upward $\Delta P_{m,t}^{up}$ and downward $\Delta P_{m,t}^{down}$ power changes can be obtained by comparing the scheduled load $P_{m,t}^{s}$ with the unscheduled load $P_{m,t}^{us}$:

$$\Delta P_{m,t}^{up} - \Delta P_{m,t}^{down} = P_{m,t}^{s} - P_{m,t}^{us} \quad (8)$$

In this formulation, the unscheduled EV charging load is used as the baseline to calculate the adopted EV energy flexibility, which further determines the remuneration for EV users.

Since EV users always tend to recharge their battery as quickly as possible, adding charging loads within the maximum EV charging power to the no-load periods will not cause inconvenience to EV users. Hence, the incentive payment $\varphi_{m,t}$ only considers downward changes $\Delta P_{m,t}^{down}$:

$$\varphi_{m,t} = \Delta P_{m,t}^{down} \gamma_m \Delta t \quad (9)$$

where γ_m is the flexibility offering price of EV user m.

When V2G operation is involved, the battery degradation cost will also be included in the payment:

$$\varphi_{m,t} = (\Delta P_{m,t}^{down} + P_{m,t}^{dis}) \gamma_m \Delta t + C_{m,t}^{bd} \quad (10)$$

where the battery degradation cost is denoted by $C_{m,t}^{bd}$. In this work, the battery degradation cost is modeled by using the battery investment cost C_m^{bi} and the total life cycles n^{lc} [40]:

$$C_{m,t}^{bd} = \frac{P_{m,t}^{dis} \Delta t}{E_m} C_m^{bi} \quad (11)$$

$$E_m = n^{lc} Cap_m \quad (12)$$

where the prospective lifetime energy output of EV m is denoted by E_m, which is given by Eq (12). Terms n^{lc} and Cap_m represent the battery life cycles and energy capacity of EV m, respectively.

III. PROBLEM FORMULATION

This section firstly presents the day-ahead CS scheduling and VPP offering problems, then gives the real-time VPP-CSs cooperative balancing problem.

A. CS Day-Ahead Scheduling

For CSs, both the market price and EV charging demand uncertainties need to be considered in the day-ahead CS scheduling problem. In this work, the market price is modeled by representative scenarios, and the EV charging demand is modeled using confidence intervals. Hence, the day-ahead scheduling problem for CSs is formulated as a stochastic minimax regret problem based on the forecasts. In stochastic minimax regret problems, the expected maximum regret is minimized under both market price and EV charging demand uncertainties:

$$\min_{P_{n,t}^{DA,cs}} \sum_{t\in 1:24} \left\{ f^{DA}(P_{n,t}^{DA,cs}) + \max_{u_t^{cs}} \left\{ \sum_{j\in J} \pi_j \min_{P_{n,t}^{cs,u}, P_{n,t}^{d,u}, P_{n,t}^{d}} [f^d(P_{n,t}^{d}) - f^{DA}(P_{n,t}^{DA,cs,u}) - f^d(P_{n,t}^{d,u})] \right\} \right\} \quad (13)$$

$$f^{DA}(P_t^{DA}) = \lambda_{t,j}^{DA,f} P_t^{DA} \quad (14)$$

$$f^d(P_t^d) = \begin{cases} |P_t^d| \lambda_t^{D+}, P_t^d \ge 0 \\ -|P_t^d| \lambda_t^{D-}, P_t^d \le 0 \end{cases} \quad (15)$$

s.t.

$$(1) - (4), (6) \quad (14)$$

$$P_{n,t}^{DA,cs} + P_{n,t}^{d} = u_t^{cs} \quad (17)$$

$$P_{n,t}^{DA,cs,u} + P_{n,t}^{d,u} = u_t^{cs} \quad (18)$$

$$(1 - \sigma^{cs}) f v_{n,t}^{cs} \le P_{n,t}^{DA,cs} \le \min\{(1 + \sigma^{cs}) f v_{n,t}^{cs}, P_{cap,n}^{cs}\} \quad (19)$$

$$\pi_1 + \pi_2 + \cdots \pi_J = 1 \quad (20)$$

where $P_{n,t}^{DA,cs}$ and $P_{n,t}^{d}$ represent the energy procurement and energy deviation of CS n at time t, respectively. Correspondingly, the optimal CS solutions under the charging demand scenario u_t^{cs} are represented by $P_{n,t}^{DA,cs,u}$ and $P_{n,t}^{d,u}$, respectively. The probability of price scenario j is given by π_j. Functions $f^{DA}(P_t^{DA})$ and $f^d(P_t^d)$ are the day-ahead energy procurement cost and energy deviation cost, respectively.

Constraints (17) and (18) are energy-balancing constraints. Constraint (19) provides a reasonable range for energy procurements to reduce the searching domain without affecting optimality. Constraint (20) ensures that the summation of all scenario probabilities equals to one.

After CSs complete their day-ahead energy procurement scheduling, the scheduling results $P_{n,t}^{DA,cs}$ of each CS n are reported to the VPP to form an aggregated VPP-CSs offering strategy in the day-ahead energy market.

B. VPP Day-Ahead Offering

In the day-ahead stage, after collecting the CS energy scheduling plans, the VPP needs to develop an aggregated offering strategy confronting price and renewable uncertainties. Based on the forecast information, the offering problem of the VPP is divided into two levels to handle these uncertainties. In the upper level, different price scenarios are generated as the inputs of the lower-level problem to acquire several price-quantity pairs for constructing offering curves. In the lower-level problem, the VPP optimizes the offering quantity and thermal productions for each forecast market price scenario $\lambda_{t,j}^{DA,f}$ under renewable output uncertainty. At the lower level, the VPP offering problem is formulated as minimax regret optimization problems. In the minimax regret problems, the maximum regret of the worst-case renewable generation is minimized for a given market price scenario $\lambda_{t,j}^{DA,f}$ at time t:

$$\min_{P_t^{DA}, P_{i,t}^{g}} \left\{ [\sum_{i\in I} f^g(P_{i,t}^{g}) - f^{DA}(P_t^{DA})] + \max_{u_t^r} \left\{ \min_{P_t^{DA,u}, P_{i,t}^{g,u}, P_t^{d,u}, P_t^{d}} [f^d(P_t^d) - \sum_{i\in I} f^g(P_{i,t}^{g,u}) + f^{DA}(P_t^{DA,u}) - f^d(P_t^{d,u})] \right\} \right\} \quad (21)$$

$$f^g(P_{i,t}^{g}) = c_i (P_{i,t}^{g})^2 + b_i P_{i,t}^{g} + a_i \quad (22)$$

s.t.

$$(1) - (5), (14), (15) \quad (23)$$

$$P_t^{d,u} + \sum_i P_{i,t}^{g,u} + u_t^r - \sum_{n\in N} P_{n,t}^{DA,cs} = P_t^{DA,u} \quad (24)$$

$$P_t^d + \sum_i P_{i,t}^g + u_t^r - \sum_{n\in N} P_{n,t}^{DA,cs} = P_t^{DA} \quad (25)$$

$$y_i^u P_{i,min}^g \le P_{i,t}^{g,u} \le y_i^u P_{i,max}^g \quad (26)$$

$$y_i P_{i,min}^g \le P_{i,t}^g \le y_i P_{i,max}^g \quad (27)$$

$$[y_i^u, y_i] \in (0,1) \quad (28)$$

where P_t^{DA}, $P_{i,t}^g$, P_t^d and u_t^r represent the market offering energy, the energy production of thermal power plant i, balancing market energy deviation, and renewable production at time t, respectively. Similarly, terms with a superscript u, including $P_t^{DA,u}$, $P_{i,t}^{g,u}$, and $P_t^{d,u}$, are the optimal VPP solutions under the scenario u_t^r. The binary variables $[y_i^u, y_i]$ are the on/off status indicators of the thermal generators. Term $P_{n,t}^{DA,cs}$ is the reported day-ahead energy procurement of CS n at time t. The thermal generator fuel cost is given by $f^g(P_{i,t}^g)$ in (22).

Constraints (24) and (25) are energy-balancing constraints. Constraints (26) to (27) are the power limit and unit commitment constraints of the thermal generators.

In the upper level, several price scenarios $j \in J$ are generated as inputs of the problem (21) – (28). After solving the lower-level minimax regret offering problem J times with different price scenarios, several optimal offering quantities can be obtained. To construct the VPP-CSs day-ahead offering curves, these optimal offering quantities are paired with the corresponding price scenarios to form price-quantity pairs as the building blocks of offering curves.

Notably, in the day-ahead stage, to keep consistent with the market-clearing resolution, the scheduling time interval for the thermal power plants, renewable power plants, and CSs is set to be one hour.

C. Cooperative VPP-CSs Real-Time Balancing

In the real-time stage, the VPP-CSs system needs to balance energy deviations resulting from the forecast errors to minimize the total cost. In the real-time stage, the market has been cleared, the connected EV charging information becomes available, and the EV charging/discharging load can be controlled by the EV charging stations. Hence, the only uncertainty remaining in this stage is renewable energy production. Besides, The EV energy scheduling problem should keep updated with EV charging information to meet the energy requirements of each EV. Therefore, the real-time VPP-CSs coordinated balancing problem is formulated as a rolling horizon optimization problem to handle the constantly updated EV charging information and renewable production forecast. Notably, to keep pace with the updated EV charging and renewable forecast information, only the first step in the solution of each scheduling horizon will be implemented. Hence, a real-time rolling horizon optimization problem needs to be solved for every scheduling period. In the real-time rolling horizon optimization model, to keep pace with the constantly updated EV charging and renewable forecast information, the optimization horizon is set to be 8 hours, and the scheduling resolution is set to be 15 minutes [19], [41]. That is, in the real-time stage, the scheduling horizon for all energy resources is 15 minutes.

In the real-time coordinated balancing problem, the VPP-CSs system simultaneously schedules the generator generation and EV charging/discharging power to minimize the total system costs, which include the fuel cost, EV user incentive cost, and energy deviation cost.

$$\min_{P_{i,t}^g, P_t^{d,vc}, \Delta P_{m,t}^{down}, \Delta P_{m,t}^{up}, P_{m,t}^{dis}} \{\sum_{t\in T}[\sum_{i\in I} f^g(P_{i,t}^g) + f^d(P_t^{d,vc}) + \sum_{m\in M} \varphi_{m,t}]\} \quad (29)$$

s.t.

$$(1) – (4), (7) – (12), (15), (22), (27), (28) \quad (30)$$

$$P_t^{DA} - \sum_{n\in N} P_{n,t}^{DA,cs} = \sum_{i\in I} P_{i,t}^g + fv_t^{r,rt} + P_t^{d,vc} - \sum_{m\in M}\left[\frac{P_{m,t}^{us} + \Delta P_{m,t}^{up} - \Delta P_{m,t}^{down}}{\eta} - \eta P_{m,t}^{dis}\right] \quad (31)$$

$$RD_i \le P_{i,t}^g - P_{i,t-1}^g \le RU_i \quad (32)$$

$$-P_m^{dis,max} \le P_{m,t}^{us} + \Delta P_{m,t}^{up} - \Delta P_{m,t}^{down} - P_{m,t}^{dis} \le P_m^{max} \quad (33)$$

$$0 \le P_{m,t}^{us} + \Delta P_{m,t}^{up} - \Delta P_{m,t}^{down} \le P_m^{max} \quad (34)$$

$$\sum_{t\in T}(\Delta P_{m,t}^{up} - \Delta P_{m,t}^{down} - P_{m,t}^{dis}) = 0 \quad (35)$$

$$SOC_{m,t} = SOC_{m,t-1} + \frac{P_{m,t}^{us} + \Delta P_{m,t}^{up} - \Delta P_{m,t}^{down} - P_{m,t}^{dis}}{Cap_m}\Delta t \quad (36)$$

$$SOC_m^{min} \le SOC_{m,,t} \le SOC_m^{max} \quad (37)$$

$$\Delta P_{m,t}^{up} \times \Delta P_{m,t}^{down} = 0 \quad (38)$$

$$\Delta P_{m,t}^{up} \times P_{m,t}^{dis} = 0 \quad (39)$$

$$[\Delta P_{m,t}^{up}, \Delta P_{m,t}^{down}, P_{m,t}^{dis}] \ge 0 \quad (40)$$

where the entire scheduling horizon is given by T. The energy deviation of the VPP-CSs system at time t is denoted by $P_t^{d,vc}$. The real-time renewable production forecast at time t is given by $fv_t^{r,rt}$. The reduced charging power, the increased charging power, and the discharged power of EV m at time t are given by $\Delta P_{m,t}^{down}$, $\Delta P_{m,t}^{up}$, and $P_{m,t}^{dis}$, respectively. The charging and discharging efficiency are given by η. Parameters RD_i and RU_i denote the ramp-down and ramp-up capabilities of thermal power plant i. The power limits of EV m are given by P_m^{max} and $P_m^{dis,max}$, respectively.

Constraint (31) is the energy-balancing constraint. The thermal power plant ramping capability is restricted by constraint (32). Constraints (33) and (34) limit the EV power. Constraint (35) ensures that the EVs are fully charged within the parking duration. Constraints (36) and (37) are the SOC constraints of EVs. Constraints (38) – (40) guarantee the rationality of the optimization results.

The solution methodology for day-ahead minimax regret problems can be referred to [42][43]. As a mixed-integer quadratic programming problem, the real-time balancing problem can be readily solved by commercial solvers such as GUROBI [44]. Besides, to efficiently solve the real-time scheduling problem for large EV fleets, the distributed solution approach [41] based on the ADMM algorithm is applied. Hence, the solution methodology to the formulated optimization problems is not provided in this paper.

IV. PROPOSED COST ALLOCATION METHOD

This section first develops a τ-value cost allocation method, then proposes a maximum right cost estimation approach to reduce the computational burden of calculating the τ-values.

A. τ-Value Cost Allocation

The VPP and CSs work cooperatively to minimize the total cost, which includes the thermal generator fuel cost, the EV user incentive cost, and the energy deviation cost. Because the VPP and CSs have different ownerships, a fair cost allocation mechanism to share the total cost among the players is the key to stabilize this VPP-CSs coalition. In this sub-section, a τ-

value method is developed to solve the cooperative game problem and allocate the costs among players.

In this cooperative game problem, the VPP and CSs represent the players in the game. That is, each stakeholder is a player in the game. The goal of this game is to analyze the contributions of each stakeholder and allocate the cost to the VPP and CSs based on their contributions.

Firstly, the VPP-CSs system is considered as a grand coalition Z. In this grand coalition, each player corresponds to a VPP or a CS. Besides, the cost generated from any sub-coalition $S \in Z$ is defined as the characteristic function $v: 2^Z \rightarrow R$ with $v(\emptyset) = 0$. Then, a cooperative game can be defined as the ordered pair $\langle Z, v \rangle$, in which the real number $v(S)$ represents the cost generated from the members of S when they cooperate.

In this cooperative game $\langle Z, v \rangle$, for each player $l \in Z$ in the sub-coalition $S: \{S \in Z, l \in S\}$, the marginal cost contribution $M_l(S, v)$ of player l to the coalition S is:

$$M_l(S, v) = v(S) - v(S \backslash \{l\}) \tag{41}$$

where the last term represents the cost generated by the rest members of S without player l. When the considered sub-coalition is the grand coalition Z, this marginal contribution of player l is defined as its utopia cost $M_l^u(Z, v)$:

$$M_l^u(Z, v) = v(Z) - v(Z \backslash \{l\}) \tag{42}$$

The utopia cost represents the cost contribution of a considered player to the total cost of the grand coalition. Namely, when a new player is added to the grand coalition, the utopia cost of the added new player is the increment of the total grand coalition cost due to the addition of this new player. The utopia cost $M_l^u(Z, v)$ is the minimum cost player l should pay. Because if player l wants to pay less, then it is more advantageous for other players in the grand coalition Z to remove player l. Hence, the utopia cost $M_l^u(Z, v)$ provides a lower bound of the cost allocated to player l. Next, an upper bound of the cost allocated to player l is found by identifying the maximum cost player l should pay.

The remainder $R(S, l)$ of player l in a sub-coalition S is defined as the cost remanent for player l in the coalition S if all other players $h: \{h \in S, h \neq l\}$ only pay their utopia costs:

$$R(S, l) = v(S) - \sum_{h \in S \backslash \{l\}} M_h^u(Z, v) \tag{43}$$

Then, for each $l \in Z$, the maximum right cost $M_l^{mrc}(v)$ is defined as the minimum remainder player l can have from all possible sub-coalitions that contain player l:

$$M_l^{mrc}(v) = \min_{S: l \in S} R(S, l) \tag{44}$$

The maximum right cost of player l is the maximum cost player l needs to pay in the grand coalition. Because if player l pays more than $M_l^{mrc}(v)$, then the sub-coalition S with $R(S, l) = M_l^{mrc}(v)$ would form a more solid coalition by making all other players in S pay their utopia costs. Hence, $M_l^{mrc}(v)$ can serve as an upper bound of the cost allocated to the player l.

After obtaining the utopia costs and maximum right costs, the lower and upper bounds of costs allocated to the VPP and each CS can be determined. With these upper and lower bounds, it is reasonable to find a compromise between the lower and upper bounds to be the solution for the cost allocation problem. By using the lower and upper bounds of costs allocated to players, the τ-values for each player $l \in Z$ can be computed such that each player pays a cost that lies between their lower and upper cost bounds:

$$\tau_l(v) = \alpha M_l^{mrc}(v) + (1 - \alpha) M_l^u(Z, v) \tag{45}$$

where the coefficient $\alpha \in [0,1]$ can be uniquely determined by satisfying the efficiency criterion:

$$\sum_{l \in Z} \tau_l(v) = v(Z) \tag{46}$$

In the cost allocation problem, the obtained τ-value $\tau_l(v)$ for player l is the cost allocated to that player.

Notably, the stakeholders in the cooperative game problem only include the VPP and CSs. Thus, the cost allocation method only handles the cost allocation problem between the VPP and CSs. For EV users, they participate in the scheduling process through the proposed incentive program, and their contributions are rewarded through the incentive program. Hence, EV users are not included in the cost allocation problem.

B. Proposed Maximum Right Cost Estimation Approach

In the conventional τ-value method, computing the maximum right costs requires evaluating the characteristic function $v: 2^Z \rightarrow R$ for 2^Z times, which is unrealistic for the considered cost allocation problem. To keep the computational burden under control, an estimation method is proposed to use fewer coalition samples to estimate the maximum right costs. By utilizing some characteristics in the τ-value calculation process, the proposed estimation approach can reduce the number of evaluated coalitions from two dimensions, including reducing the number of players considered for sampling and reducing the number of considered coalition sizes.

The first attempt to reduce the computational burden is to reduce the number of considered players. When calculating the remainder $R(S, l)$ for player l in coalition S, the decisive factors include the utopia costs $M_h^u(Z, v)$ of other players and the total cost $v(S)$ generated from coalition S. Hence, it is straightforward to imply that smaller remainders for player l can be achieved with smaller total costs $v(S)$ and larger utopia costs $M_h^u(Z, v)$ of other players in the coalition S. Based on this implication, the attractiveness $Attractiveness(h, l)$ of player h to player l is defined as the opposite of $R(S, l)$, in which the coalition S only consists of players l and h:

$$Attractiveness(h, l) = M_h^u(Z, v) - v(l + h) \tag{47}$$

The attractiveness $Attractiveness(h, l)$ serves as a measure of how attractive it is for player l to cooperate with player h. The less player l needs to pay by cooperating with player h, the more attractive player h is to player l. By evaluating all two-member coalitions, one can obtain an attractiveness matrix $AttM$ that records the attractiveness of all players to other players in the grand coalition. With the attractiveness matrix, the coalition sampling for calculating the maximum right costs can be more instructive. That is, when choosing members to form coalitions with player l, one can selectively consider those players with large attractiveness $Attractiveness(h, l)$ to player l.

To select attractive players to form coalitions with player l, players $h \in Z/\{l\}$ are ordered based on their attractiveness to player l. In the decreasingly ordered list $OAttM_l = \{h_1^l \dots h_k^l \dots h_{Z-1}^l\}$, the kth element h_k^l is the kth attractive member to player l. Then, the players that will be selected for sampling can be shortlisted by finding a number K, which determines how many players will be considered when estimating the maximum right cost for player l. The number of considered shortlisted players is constrained by the value of K. More specifically, only the first K attractive players in $OAttM_l = \{h_1^l \dots h_k^l \dots h_{Z-1}^l\}$ will be considered to form coalition samples with player l. Setting the value of K is meant to filter out the members that are less likely to yield better maximum right cost estimations, which can reduce the computational burden for estimation.

On the one hand, increasing K can increase the sampling domain, which may provide closer estimations of the actual maximum right costs. On the other hand, a larger K will increase the computational burden by enlarging the sampling domain. Hence, it is of vital importance to find a proper value of K to meet the estimation accuracy requirements while avoiding unbearable computational burdens. In the proposed estimation approach, the optimal value of K can be uniquely determined by the number of considered coalition sizes, as will be shown later in Eq (49).

The number of considered coalition sizes is another factor that can affect the computational burden for estimating the maximum right costs. Considering more coalition sizes will increase the computational burden. The process of determining the minimum number of considered coalition sizes is given next.

For each player l, coalitions with increasing sizes are formed by gradually adding members according to $OAttM_l$. Meanwhile, the remainder for player l under each coalition size $|S|$ is recorded to generate a remainder matrix $RM(l,|S|)$. In each row of the remainder matrix $RM(l,|S|)$, the global minimum remainder for player l can be found. For different coalition sizes, the difference between the global minimum remainder and the local minimum remainder found before this coalition size can shed some light on the maximum right cost estimation accuracy because the true maximum right cost is the global minimum remainder obtained from a larger coalition sample domain. Hence, to determine the number of coalition sizes for evaluation, one only needs to identify a maximum coalition size $|S|_{max}$, such that for all players $l \in Z$, the maximum deviation between the global minimum remainder and the local minimum remainder found before this coalition size is below the given accuracy threshold ε:

$$\max_{l\in Z}\left\{\frac{\min[RM(l,|S|\le|S|_{max})]}{\min[RM(l,|S|\le Z)]}-1\right\}\le\varepsilon \tag{48}$$

After identifying the maximum evaluated coalition size $|S|_{max}$, the optimal value of K can be determined by (49).

$$K=|S|_{max}-1 \tag{49}$$

The optimal value of K is given by (49) because the considered player l must be included in all sampled sub-coalitions, and at least $(|S|_{max}-1)$ extra members are needed to from a sub-coalition with size $|S|_{max}$.

After determining K and $|S|_{max}$, one can estimate the maximum right cost for player l by evaluating all possible coalitions S_{sample} that can be formed by player l and members in $\{h_1^l, h_2^l \dots h_K^l\}$:

$$estM_l^{mrc}(v)=\min_{S_{sample},l\in S_{sample}} R\left(S_{sample},l\right) \tag{50}$$

where $estM_l^{mrc}(v)$ represents the estimated maximum right cost for player l. To this end, the estimated τ-values for each player can be obtained by replacing the $M_l^{mrc}(v)$ in (45) with $estM_l^{mrc}(v)$.

The proposed estimated τ-value cost allocation method can be summarized as follows:

Step 1: Set the remainder deviation threshold ε.

Step 2: Calculate the utopia costs for all players $l \in Z$.

Step 3: Derive the attractive matrix $AttM(h,l)$ and create the ordered list $OAttM_l$ for each player.

Step 4: Derive the remainder matrix $RM(l,|S|)$.

Step 5: Obtain the considered coalition size $|S|_{max}$, derive shortlisted member size K through (48) and (49).

Step 6: For each player l, evaluate all possible coalitions formed by l and members in $\{h_1^l, h_2^l \dots h_K^l\}$, derive the estimated maximum right costs for all players from (50).

Step 7: Obtain the estimated τ-values from (45) and (46) and allocate the cost based on the estimated τ-values.

The flowchart for applying the estimated τ-value cost allocation method is summarized in Fig. 4.

Under the proposed estimation approach, the maximum number of required evaluations N_{max}^{eval} is reduced from 2^Z to:

$$N_{max}^{eval}=C_Z^2+(Z^2-3Z+1)+Z\sum_{|S|=3}^{|S|_{max}}C_K^{|S|-1} \tag{51}$$

where the first term is for deriving the attractiveness matrix $AttM(h,l)$. The second term is for developing the remainder matrix $RM(l,Z)$ and utopia costs $M_h^u(Z,v)$. The third term is for estimating other possible coalitions. Notably, (51) only gives a theoretical upper bound for the number of required evaluations. When applying the proposed estimation approach, the sampled coalitions for estimating the maximum right costs may overlap with each other, and these repeatedly sampled coalitions only need to be evaluated once. Besides, based on (51), as more players join this coalition, the computational complexity of the proposed cost allocation method becomes $O(n^2)$, whereas the computational complexity of the conventional τ-value method is $O(2^n)$.

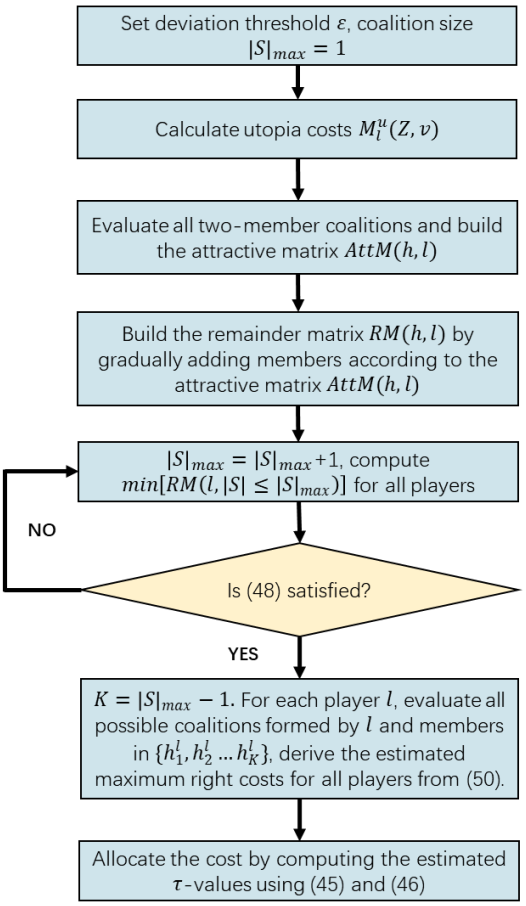

Fig. 4. Flowchart of the estimated τ-value cost allocation method.

V. CASE STUDY

A. Basic Data

The considered VPP-CSs system consists of a distributed generator-based VPP and 10 CSs. The generator parameters are given in Table I. The day-ahead forecast renewable generation [45] and market price scenarios [46] are presented in Fig. 5, which are generated from ARIMA models [42] by using

historical data. The market penalty coefficients are set to $\omega^- = 0.5$ and $\omega^+ = 1.5$ to moderately penalize the energy deviations. Fig. 5b also shows the forecast CS load profiles generated by using the k-means scenario reduction method [47]. Negative CS loads in Fig. 5b suggest that CSs would discharge the EVs at those high average forecast price periods. The number of price scenarios generated to construct the offering curves is set to five. Uncertainty coefficients σ^r and σ^{cs} are set to 0.3.

Table I
GENERATOR CHARACTERISTICS

	P_{max} (MW)	$EcoP_{min}$ (MW)	RU (MW/h)	RD (MW/h)	a $\$/h$	b $\$/MWh$	c $(\$/MWh)^2$
TP 1	9	1	3	3	120	40	1.10
TP 2	7	1	2.5	2.5	100	45	1.15
TP 3	5	1	2	2	80	50	1.20
WP	6	0	/	/	/	/	/

TP: thermal power plant; WP: wind power plant

In the real-time stage, the scheduling horizon is set to 8 hours with a scheduling resolution of 15 minutes [19]. The real-time EV charging data is obtained from [30]. It is assumed that the number of EVs charging in each CSs follows the uniform distribution $U(160,240)$. In total, 2,031 EVs are generated for the considered 10 CSs. The EV user offering prices γ_m for energy flexibility are assumed to follow the normal distribution with mean and variance equal to half of the average market energy prices. The EV charging price is set to 1.5 times of the average day-ahead energy market price. The charging and discharging efficiency of EVs is set to be 0.95. In the cost allocation stage, the remainder deviation threshold ε is set to be 0.01.

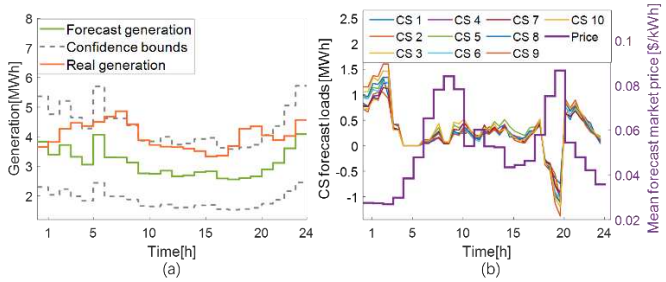

Fig. 5. (a) day-ahead renewable generation information, (b) forecast CS load profiles and average forecast market price

B. *Numerical Results*

Fig. 6 gives several typical offering curves from the VPP-CSs system and the day-ahead market-clearing results. The offering curves in Fig. 6a correspond to low (hour 5), medium (hour 14), and high (hour 18) average forecast prices, respectively. In hour 5, the VPP-CSs system decides not to turn on the thermal power plants for some low-price scenarios, making the first three steps offer the same energy in the market. Thus, the offering curve for hour 5 only has three price-quantity pairs. In hour 14, the forecast price scenarios are distributed in a range that allows the VPP-CSs system to offer a different quantity at each price scenario, leading to a five-step offering curve for hour 14. Hour 18 has high forecast prices, making it offer at full capacity for the last two price scenarios. Thus, only four price-quantity pairs are observed in that offering curve.

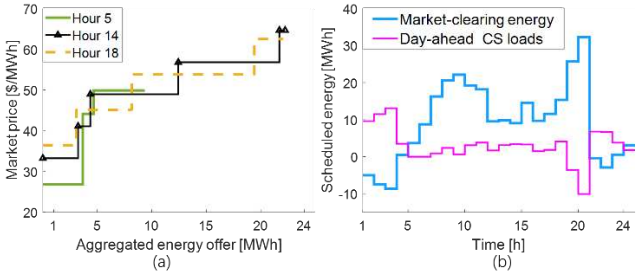

Fig. 6. (a) typical offering curves, (b) day-ahead scheduling results

The day-ahead market-clearing results are presented in Fig. 6b together with the total scheduled day-ahead CS loads. Due to low average forecast prices, the aggregated VPP-CSs loads are negative in hours 1 to 4, suggesting that the considered VPP-CSs system is a consumer that imports energy from the grid. When forecast prices are high enough, to maximize the total profit, the VPP-CSs system not only offers its energy generation but also offers discharged EV energy to the market, such as in hours 19 and 20. In some hours, the market energy exchange is nearly zero, because the generated energy is used to satisfy EV charging demands, such as hours 4, 21, and 23.

The revenues and costs of the VPP-CSs system are shown in Fig. 7. The revenues include the day-ahead market revenue, EV charging revenue, and the balancing market revenue when there is an energy surplus. The costs include fuel costs, EV incentive costs, EV energy discharging costs, and balancing market costs when there is an energy deficiency. The largest revenue comes from the day-ahead market, which is \$16,366 in total. The revenue for charging EVs is \$5,930. Because the forecast renewable power generation is much lower than the actual renewable power output, the total balancing cost is \$-650, which suggests that the VPP-CSs system is earning money from the balancing market under the dual pricing rule. The largest cost of the VPP-CSs system is the fuel cost, which is \$11,251 in total. The total EV incentive cost is \$964, which is mostly concentrated at high-price hours 19 and 20. Throughout the operating day, each EV user gets an average incentive payment of \$0.475, which is 16.3% of their average charging cost (\$2.920). Overall, the net profit of the VPP-CSs system over the day is \$10,731.

The VPP load profile and revenue are also displayed in Fig. 7. In Fig. 7, there are some mismatches between the VPP revenue and the VPP load profile. For example, the VPP produces the most energy in hour 10, whereas its revenue in hour 10 is not the highest. Such mismatches are caused by the energy prices in the electricity market. Due to the volatile energy prices, producing the same energy may lead to different VPP revenues.

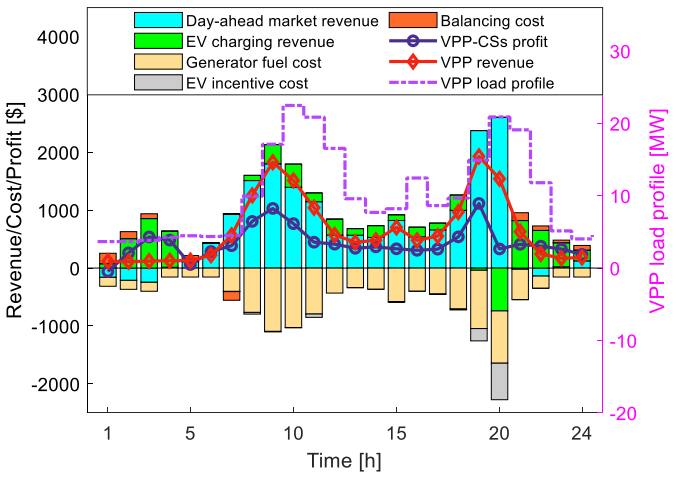

Fig. 7. Optimization results of the VPP-CSs system

Define the τ-value estimation accuracy θ_l for player l as (52), the average estimation accuracy by using the proposed estimated τ-value method can reach 99.2%.

$$\theta_l = 1 - \sqrt{\left(\frac{\tau_l^{est} - \tau_l^{conv}}{\tau_l^{conv}}\right)^2} \tag{52}$$

where τ_l^{est} and τ_l^{conv} are τ-values of player l obtained from the estimated and conventional τ-value methods, respectively.

By applying the estimated τ -value method and the conventional τ-value method, the profits of each player in the VPP-CSs system are displayed in Fig. 8a. In Fig. 8a, the results obtained from the estimated and conventional τ-value methods are very close to each other, which further confirms that the proposed method can achieve accurate estimations.

To prove the performance of the proposed cooperative VPP-CSs operation framework, the profits of the non-cooperative case (VPP and each CS operate separately) are displayed in Fig. 8b. The VPP profit increment is \$400.8 as compared to the case of no cooperation (\$8,700.2). The CS profit increments are distributed from \$8.4 to \$37.4 with an average value of \$27.9. Considering that the average CS profit without cooperation is \$135.1, the average CS profit is increased by 20.7% through the proposed cooperative operation. As compared to the non-cooperation case, the proposed cooperative framework increases the total profit of the VPP-CSs system by 6.8% (from \$10,051 to \$10,731).

To further confirm the benefits of CSs in collaborating with the VPP, the case in which the CSs form a coalition without involving the VPP (semi-cooperative, case 2) is also investigated. The results are presented in Table II together with the non-cooperative case (VPP and each CS operate separately, case 1) and the proposed cooperative framework (case 3). Notably, the data in Table II is the aggregated result of both the VPP and CSs.

Comparing case 2 with case 1, the cooperation among CSs can moderately reduce the total balancing cost of CSs, and the incentive payment remains almost the same. Hence, in the semi-cooperative case, the profit increment mainly comes from the cross-balancing effect among the CSs. When VPP is involved in the coalition, on the one hand, the cross-balancing effect is more significant. On the other hand, the VPP can absorb the CS deviations at lower costs by using its generation flexibility, hence, reducing both the balancing cost and the EV incentive cost. Consequently, in the cooperative case, the involvement of the VPP can bring a huge benefit to CSs, as shown in Table II.

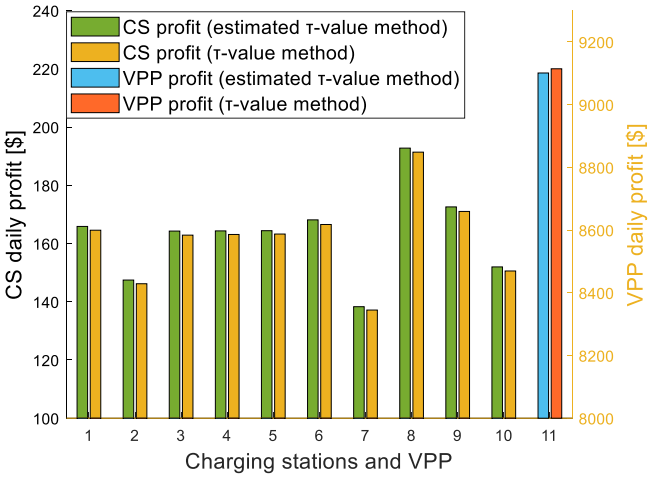

(a)

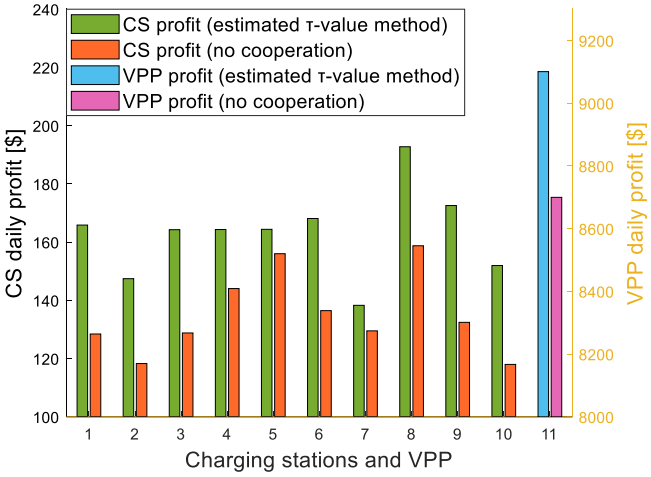

(b)

Fig. 8. (a) Profits using the estimated τ-value method and standard τ-value method, (b) profits using the estimated τ-value method and under no cooperation.

Notably, it is assumed that CSs can participate in the wholesale market in all cases. Whereas in practical scenarios, CSs are generally not allowed to access the wholesale market due to their small capacities. In that case, they must face higher electricity prices from the distribution network operator.

TABLE II
COMPARISON OF DIFFERENT COOPERATIVE LEVELS

	Deviation cost [$]	Incentive cost [$]	CS profit [$]	VPP profit [$]	Total profit [$]
Non-cooperative	-401	1,397	1350.8 (100%)	8700.2 (100%)	10,051 (100%)
Semi-cooperative	-523	1,398	1472.8 (109.0%)	8700.2 (100%)	10,173 (101.2%)
Cooperative	-650	964	1630.0 (120.7%)	9101.0 (104.6%)	10,731 (106.8%)

To verify the superiority of the proposed incentive program, four incentive programs are evaluated in this work. Program 1 is the benchmark incentive program proposed in [30], in which the V2G operation is not considered, and the uniform pricing mechanism is used. In program 2, the V2G operation is added

on top of the benchmark program. In program 3, the uniform pricing in the benchmark program is replaced with the pay-as-bid mechanism. Program 4 is the proposed incentive program, which concurrently adopts the V2G operation and the pay-as-bid rule. The optimization results of different programs are summarized in Table III.

TABLE III
COMPARISON OF DIFFERENT INCENTIVE PROGRAMS

VPP-CSs system	Benchmark	With V2G	With pay-as-bid	Proposed
Total revenue [$]	21,211	21,494	21,715	22,296
Total cost [$]	10,928	11,113	11,123	11,565
Total profit [$]	10,283 (100%)	10,381 (100.9%)	10,592 (103.0%)	10,731 (104.4%)
Incentive Payment [$]	489	716	630	964
Adopted energy flexibility [kWh]	15,686	20,774	22,114	30,090

By comparing program 2 with the benchmark, one can observe that with the V2G operation, the profit of the VPP-CSs system is increased by $98, and the incentive payment for EV users is increased by $227. These economic benefits are generated by adopting EV discharging energy flexibility through the V2G operation. The advantage of the pay-as-bid rule is demonstrated by comparing program 3 with the benchmark. In program 3, the pay-as-bid rule allows 6,428 kWh more EV energy flexibility to be adopted as compared to the uniform pricing mechanism, suggesting that the pay-as-bid rule is more efficient in encouraging the utilization of EV energy flexibility. With an increased EV energy flexibility utilization rate, the total profit of the VPP-CSs system and the total incentive payment for EV users are increased by $309 and $141, respectively. When both the V2G operation and pay-as-bid are considered, as in the proposed incentive program, the incentive payment for EV users almost doubled (from $489 to $964). For the VPP-CSs system, its total profit is also increased by $448, which is 4.4% of its total profit. Besides, by using the proposed incentive program, the adopted EV energy flexibility is almost twice of the adopted EV energy flexibility from the benchmark, which confirms its superiority in encouraging the utilization of EV energy flexibility.

C. τ-Value Estimation

This sub-section provides some analysis of the proposed estimation approach. The obtained attractiveness matrix is displayed in Fig. 9. In Fig. 9a, the VPP is set to be player 1, and CSs are set to be players 2 to 11. As shown in Fig. 9a, the attractiveness of CSs to the VPP is much smaller than their attractiveness to other CSs. This is because the VPP has much larger remainders than CSs in all cases. Besides, the VPP's attractiveness to other CSs is also obviously lower than the attractiveness of CSs to other CSs. This is because the utopia cost of the VPP is much lower than the total cost of any two-player coalition that includes the VPP and a CS. To show the variance of the attractiveness matrix more clearly, the rest part of the attractiveness matrix without the VPP is displayed in Fig. 9b, which shows that the attractiveness between different players can be very different. Fig. 9b also gives straightforward information on which players are more attractive to the considered player when estimating the maximum right cost for player l. Notably, in the diagonals of Fig. 9, the attractiveness is not displayed because they represent one-member coalitions.

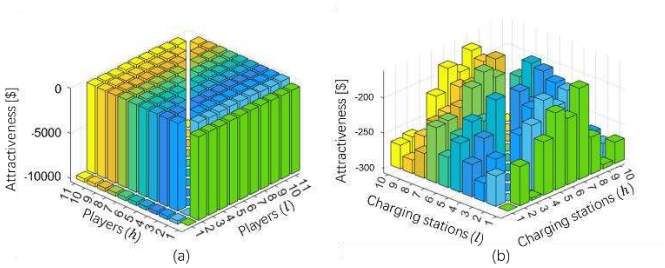

Fig. 9. Attractive matrix for (a) all players and (b) CSs only.

The remainders for all players under different coalition sizes are shown in Fig. 10. Fig. 10a displays the remainders for the VPP. One can observe that the remainder for the VPP gradually decreases with increasing coalition sizes until coalition sizes 10 and 11, in which the VPP remainder reaches $10,238.9. Besides, Fig. 10a also shows that with increasing coalition sizes, the VPP remainder drops most significantly when coalition sizes are small, which suggests that cooperation with more attractive CSs can give more remainder drops for the VPP. The remainders of CSs are shown in Fig. 10b, which tells that the remainders of CSs are always increasing with enlarged coalition sizes. Hence, the global minimum remainders of CSs are all obtained by forming two-member coalitions consist of CS l and its most attractive player h_1^l.

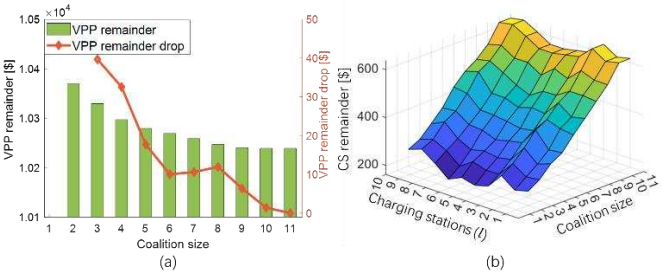

Fig. 10. (a) Remainders and remainder drops for the VPP, (b) remainders for CSs.

The ratios between the estimated τ-values and the actual τ-values under different $|S|_{max}$ and K are displayed in Fig. 11. In Fig. 11, the VPP is player 1, and CSs are players 2 to 11. Because $|S|_{max}$ is uniquely related to K, only K is used to represent each $|S|_{max}$ and K combination. As shown in Fig. 11, when $K = 2$, the maximum deviation of the estimated τ-value from the true τ-value is about 2%. The τ-value estimation deviations are gradually reduced with increased coalition samples. Such deviation reduction is less significant for larger estimation sizes, suggesting that the marginal effect of considering larger coalition sizes is decreasing.

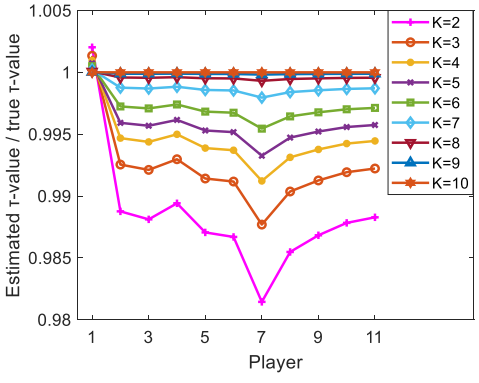

Fig. 11. Estimated deviations under different K and $|S|_{max}$.

By using the proposed τ-value estimation approach, the minimum $|S|_{max}$ and K that can satisfy this accuracy threshold are 4 and 3, respectively. In that case, the maximum number of coalitions that should be evaluated in the estimation process is N_{max}^{eval} =188, which is much less than 2,048 evaluations of the conventional τ-value method. To show the scalability of the proposed cost allocation method, the required numbers of evaluations using the conventional τ -value method, the coalitional τ-value method [48], and the proposed estimation approach are displayed in Fig. 12. In the coalitional τ-value method, it is assumed that there are three prior unions, including the VPP and two CS unions. In Fig. 12, as the coalition size grows, the conventional τ-value method becomes computationally impractical because of its exponential computational complexity. Compared with the coalitional τ-value method, the proposed estimated τ-value method suffers slightly more computational burden at small coalition sizes ($N \leq 10$). As the number of players grows, the computational burden of the coalitional τ -value method also grows exponentially, whereas the number of computations of the proposed method remains to be low.

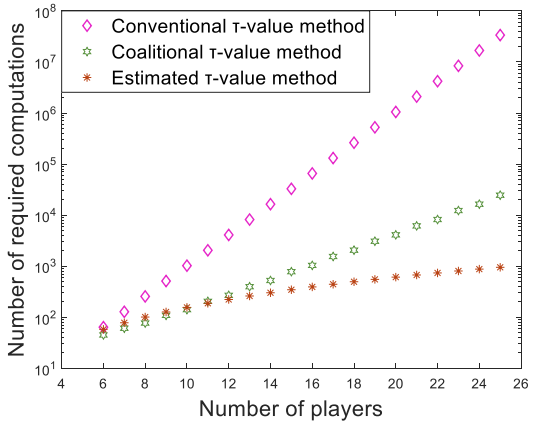

Fig. 12. Computational performance comparison.

Notably, under the distributed solution approach, the proposed methods have good scalability concerning the number of EVs. The solution time for the real-time scheduling problem is mainly affected by the CS that has the most EVs to be scheduled. Normally, it takes a few seconds to solve a single real-time scheduling problem. Besides, evaluating a single sub-coalition requires solving the real-time scheduling problem 96 times. On average, evaluating one sub-coalition takes 198.9s.

VI. CONCLUSION

This work is devoted to proposing a cooperative operation framework for VPPs and CSs that have different interests. To support the flexible operation of the considered VPP-CSs system, an EV user incentive program is proposed for acquiring EV energy flexibility. To efficiently address the conflicting interests between different stakeholders, an estimated τ-value cost allocation method is also proposed.

In the cooperative framework, the cross-balancing effect that can reduce the deviation cost is obvious among the players. To fully make use of this cross-balancing effect, large EV charging management platforms should be established to collectively manage the charging load of larger EV fleets. Besides, new electricity market products should be designed to further unleash the potential of EV energy flexibility. As compared to the case of no cooperation, the average CS profit and VPP profit have been increased by 20.7% and 4.6%, respectively, achieving a win-win situation for all members. For the proposed EV user incentive program, numerical results suggest that both the V2G operation and pay-as-bid strategy can enhance the profitability of the considered system. But the improvement from adopting the pay-as-bid strategy (3.0%) is more obvious than involving the V2G operation (0.9%). For the considered VPP-CSs system, compared to the conventional τ-value method, the proposed τ-value estimation approach can reduce the computational burden from 2047 evaluations to 188 evaluations, meanwhile, achieving an average of 99.2% estimation accuracy. As compared to the coalitional τ-value method, the proposed method can also significantly reduce the computational burden for large coalitions. The computational burden reduction of the proposed method will become more significant as the size of the coalition grows, which can be a future extension of this work.

REFERENCE

[1] R. Zhang and B. Hredzak, "Distributed Dynamic Clustering Algorithm for Formation of Heterogeneous Virtual Power Plants Based on Power Requirements," *IEEE Trans. Smart Grid*, vol. 12, no. 1, pp. 192–204, 2021.

[2] N. Naval and J. M. Yusta, "Virtual power plant models and electricity markets - A review," *Renew. Sustain. Energy Rev.*, vol. 149, p. 111393, 2021.

[3] Y. Wu, Z. Wang, Y. Huangfu, A. Ravey, D. Chrenko, and F. Gao, "Hierarchical Operation of Electric Vehicle Charging Station in Smart Grid Integration Applications — An Overview," *Int. J. Electr. Power Energy Syst.*, vol. 139, September 2021.

[4] X. Yang and Y. Zhang, "A comprehensive review on electric vehicles integrated in virtual power plants," *Sustain. Energy Technol. Assessments*, vol. 48, p. 101678, October 2021.

[5] M. H. Abbasi, M. Taki, A. Rajabi, L. Li, and J. Zhang, "Coordinated operation of electric vehicle charging and wind power generation as a virtual power plant: A multi-stage risk constrained approach," *Appl. Energy*, vol. 239, pp. 1294–1307, January 2019.

[6] L. Ju, H. Li, J. Zhao, K. Chen, Q. Tan, and Z. Tan, "Multi-objective stochastic scheduling optimization model for connecting a virtual power plant to wind-photovoltaic-electric vehicles considering uncertainties and demand response," *Energy Convers. Manag.*, vol. 128, pp. 160–177, 2016.

[7] F. MulSheidaei and A. Ahmarinejad, "Multi-stage stochastic framework for energy management of virtual power plants considering electric vehicles and demand response programs," *Int. J. Electr. Power Energy Syst.*, vol. 120, p. 106047, December 2020.

[8] A. Alahyari, M. Ehsan, and M. S. Mousavizadeh, "A hybrid storage-wind virtual power plant (VPP) participation in the electricity markets: A self-scheduling optimization considering price, renewable generation, and electric vehicles uncertainties," *J. Energy Storage*, vol. 25, p. 100812, June 2019.

[9] A. Shayegan-Rad, A. Badri, and A. Zangeneh, "Day-ahead scheduling of virtual power plant in joint energy and regulation reserve markets under uncertainties," *Energy*, vol. 121, pp. 114–125, 2017.

[10] S. Sadeghi, H. Jahangir, B. Vatandoust, M. A. Golkar, A. Ahmadian, and A. Elkamel, "Optimal bidding strategy of a virtual power plant in day-ahead energy and frequency regulation markets: A deep learning-based approach," *Int. J. Electr. Power Energy Syst.*, vol. 127, p. 106646, October 2021.

[11] M. Vasirani, R. Kota, R. L. G. Cavalcante, S. Ossowski, and N. R. Jennings, "An agent-based approach to virtual power plants of wind power generators and electric vehicles," *IEEE Trans. Smart Grid*, vol. 4, no. 3, pp. 1314–1322, 2013.

[12] D. Yang, S. He, M. Wang, and H. Pandzic, "Bidding Strategy for Virtual Power Plant Considering the Large-Scale Integrations of

Electric Vehicles," *IEEE Trans. Ind. Appl.*, vol. 56, no. 5, pp. 5890–5900, 2020.

[13] S. M. Kassi, Amitabh Kant, Randheer Singh, Sanjeev Kumar, Ashutosh Sharma, "Handbook of Electric Vehicle Charging Infrastructure Implementation," *Electr. Hybrid Veh.*, pp. 517–543, 2021.

[14] B. Behi, A. Arefi, P. Jennings, A. Gorjy, and A. Pivrikas, "Advanced monitoring and control system for virtual power plants for enabling customer engagement and market participation," *Energies*, vol. 14, no. 4, 2021.

[15] B. Zhou *et al.*, "Optimal Coordination of Electric Vehicles for Virtual Power Plants with Dynamic Communication Spectrum Allocation," *IEEE Trans. Ind. Informatics*, vol. 17, no. 1, pp. 450–462, 2021.

[16] J. Wang, C. Guo, C. Yu, and Y. Liang, "Virtual power plant containing electric vehicles scheduling strategies based on deep reinforcement learning," *Electr. Power Syst. Res.*, vol. 205, p. 107714, October 2022.

[17] S. Fan, J. Liu, Q. Wu, M. Cui, H. Zhou, and G. He, "Optimal coordination of virtual power plant with photovoltaics and electric vehicles: A temporally coupled distributed online algorithm," *Appl. Energy*, vol. 277, p. 115583, June 2020.

[18] H. Chung, S. Member, W. Li, C. Yuen, and S. Member, "Electric Vehicle Charge Scheduling Mechanism to Maximize Cost Efficiency and User Convenience," *IEEE Trans. Smart Grid*, vol. 10, no. 3, pp. 3020–3030, 2019.

[19] J. Su, T. T. Lie, and R. Zamora, "A rolling horizon scheduling of aggregated electric vehicles charging under the electricity exchange market," *Appl. Energy*, vol. 275, p. 115406, July 2020.

[20] A. Dubey, S. Santoso, M. P. Cloud, and M. Waclawiak, "Determining Time-of-Use Schedules for Electric Vehicle Loads: A Practical Perspective," *IEEE Power Energy Technol. Syst. J.*, vol. 2, no. 1, pp. 12–20, 2015.

[21] Y. Song, L. Shangguan, and G. Li, "Simulation analysis of flexible concession period contracts in electric vehicle charging infrastructure public-private-partnership (EVCI-PPP) projects based on time-of-use (TOU) charging price strategy," *Energy*, vol. 228, p. 120328, 2021.

[22] F. Sheidaei and A. Ahmarinejad, "Multi-stage stochastic framework for energy management of virtual power plants considering electric vehicles and demand response programs," *Int. J. Electr. Power Energy Syst.*, vol. 120, p. 106047, December 2020.

[23] S. M. B. Sadati, J. Moshtagh, M. Shafie-khah, A. Rastgou, and J. P. S. Catalão, "Bi-level model for operational scheduling of a distribution company that supplies electric vehicle parking lots," *Electr. Power Syst. Res.*, vol. 174, p. 105875, April 2019.

[24] Z. Liu, Q. Wu, K. Ma, M. Shahidehpour, Y. Xue, and S. Huang, "Two-Stage Optimal Scheduling of Electric Vehicle Charging Based on Transactive Control," *IEEE Trans. Smart Grid*, vol. 10, no. 3, pp. 2948–2958, 2018.

[25] Z. Liu, Q. Wu, M. Shahidehpour, C. Li, S. Huang, and W. Wei, "Transactive real-time electric vehicle charging management for commercial buildings with PV on-site generation," *IEEE Trans. Smart Grid*, vol. 10, no. 5, pp. 4939–4950, 2019.

[26] M. M. Hoque, M. Khorasany, R. Razzaghi, H. Wang, and M. Jalili, "Transactive Coordination of Electric Vehicles with Voltage Control in Distribution Networks," *IEEE Trans. Sustain. Energy*, vol. 13, no. 1, pp. 391–402, 2021.

[27] T. Zhao, Y. Li, X. Pan, P. Wang, and J. Zhang, "Real-Time Optimal Energy and Reserve Management of Electric Vehicle Fast Charging Station: Hierarchical Game Approach," *IEEE Trans. Smart Grid*, vol. 9, no. 5, pp. 5357–5370, 2018.

[28] W. Liu, S. Chen, Y. Hou, and Z. Yang, "Optimal Reserve Management of Electric Vehicle Aggregator: Discrete Bilevel Optimization Model and Exact Algorithm," *IEEE Trans. Smart Grid*, vol. 12, no. 5, pp. 4003–4015, 2021.

[29] C. Of and M. Island, "A Coordinated Dynamic Pricing Model for Electric Vehicle Charging Stations," *IEEE Trans. Transp. Electrif.*, vol. 5, no. 1, pp. 226–238, 2019.

[30] H. Wang, G. S. Member, Y. Jia, M. Shi, and S. Member, "A Hybrid Incentive Program for Managing Electric Vehicle Charging Flexibility," *IEEE Trans. Smart Grid*, vol. 14, no. 1, pp. 476–488, 2023.

[31] S. Sharma, S. Member, and A. R. Abhyankar, "Loss Allocation for Weakly Meshed Distribution System Using Analytical Formulation of Shapley Value," vol. 32, no. 2, pp. 1369–1377, 2017.

[32] Y. Li, W. Liu, M. Shahidehpour, F. Wen, K. Wang, and Y. Huang, "Optimal Operation Strategy for Integrated Natural Gas Generating Unit and Power-to-Gas Conversion Facilities," vol. 9, no. 4, pp. 1870–1879, 2018.

[33] J. Mei, C. Chen, J. Wang, and J. L. Kirtley, "Coalitional game theory based local power exchange algorithm for networked microgrids," *Appl. Energy*, vol. 239, pp. 133–141, January 2019.

[34] M. M. Rahman, A. O. Oni, E. Gemechu, and A. Kumar, "Assessment of energy storage technologies: A review," *Energy Convers. Manag.*, vol. 223, p. 113295, May 2020.

[35] E. G. Kardakos, C. K. Simoglou, and A. G. Bakirtzis, "Optimal Offering Strategy of a Virtual Power Plant: A Stochastic Bi-Level Approach," *IEEE Trans. Smart Grid*, vol. 7, no. 2, pp. 794–806, 2016.

[36] A. Alahyari, M. Ehsan, and M. S. Mousavizadeh, "A hybrid storage-wind virtual power plant (VPP) participation in the electricity markets: A self-scheduling optimization considering price, renewable generation, and electric vehicles uncertainties," *J. Energy Storage*, vol. 25, p. 100812, February 2019.

[37] B. K. Sovacool, L. Noel, J. Axsen, and W. Kempton, "The neglected social dimensions to a vehicle-to-grid (V2G) transition: A critical and systematic review," *Environ. Res. Lett.*, vol. 13, no. 1, 2018.

[38] C. Heilmann and G. Friedl, "Factors influencing the economic success of grid-to-vehicle and vehicle-to-grid applications—A review and meta-analysis," *Renew. Sustain. Energy Rev.*, vol. 145, April, 2021.

[39] B. Bibak and H. Tekiner-Moğulkoç, "A comprehensive analysis of Vehicle to Grid (V2G) systems and scholarly literature on the application of such systems," *Renew. Energy Focus*, vol. 36, pp. 1–20, March 2021.

[40] R. Das *et al.*, "Multi-objective techno-economic-environmental optimisation of electric vehicle for energy services," *Appl. Energy*, vol. 257, p. 113965, April 2020.

[41] H. Wang, M. Shi, P. Xie, C. S. Lai, K. Li, and Y. Jia, "Electric Vehicle Charging Scheduling Strategy for Supporting Load Flattening Under Uncertain Electric Vehicle Departures," vol. XX, no. Xx, pp. 1–12.

[42] H. Wang, Y. Jia, C. S. Lai, P. Xie, and M. Shi, "Two-Stage Minimax Regret-Based Self-Scheduling Strategy for Virtual Power Plants," *IEEE Power Energy Soc. Gen. Meet.*, July 2021.

[43] H. Wang, Y. Jia, C. S. Lai, and K. Li, "Optimal Virtual Power Plant Operational Regime under Reserve Uncertainty," *IEEE Trans. Smart Grid*, vol. 4, no. 13, 2022.

[44] "GUROBI optimizer [online]." https://www.gurobi.com/products/gurobi-optimizer/ (accessed Jan. 15, 2022).

[45] "FINFRID [online]." https://data.fingrid.fi/open-data-forms/search/en/?selected_datasets=181 (accessed Jun. 14, 2021).

[46] "N2EX Day Ahead Auction Prices [online]." https://www.nordpoolgroup.com/Market-data1/GB/Auction-prices/UK/Hourly/?view=table (accessed Mar. 07, 2021).

[47] M. K. Gray and W. G. Morsi, "Power quality assessment in distribution systems embedded with plug-in hybrid and battery

electric vehicles," *IEEE Trans. Power Syst.*, vol. 30, no. 2, pp. 663–671, 2015.

[48] B. Casas-Méndez, I. García-Jurado, A. Van den Nouweland, and M. Vázquez-Brage, "An extension of the τ-value to games with coalition structures," *Eur. J. Oper. Res.*, vol. 148, no. 3, pp. 494–513, 2003.

Han Wang (S'20) received the B.Sc. degree in New Energy Science and Engineering from Chinese University of Hong Kong (Shenzhen), China, in 2019. He is currently a joint PhD candidate with Southern University of Science and Technology, China, and The University of Leeds, UK. His research interests include virtual power plants, electric vehicle fleets, microgrids, energy management, power system optimization, and artificial intelligence application in power system.

Youwei Jia (S'11, M'15) received the B.Eng and Ph.D degrees from Sichuan University, China, in 2011, and The Hong Kong Polytechnic University, Hong Kong, in 2015, respectively. From 2015 to 2018, he was a postdoctoral fellow at The Hong Kong Polytechnic University. He is currently an Assistant Professor with the Department of Electrical and Electronic Engineering, University Key Laboratory of Advanced Wireless Communication of Guangdong Province and Shenzhen Key Laboratory of Electrical Direct Drive Technology, Southern University of Science and Technology, Shenzhen, China.

His research interests include microgrid, renewable energy modeling and control, power system security analysis, complex network and artificial intelligence in power engineering.

Mengge Shi (S'22) received the B.Eng and M.Eng degrees from Changsha University of Science and Technology, China, in 2019, and Southern University of Science and Technology, China, in 2022, respectively. She is currently a Ph.D candidate with Southern University of Science and Technology, China. Her research interests include integrated energy system energy management, smart buildings, and electric vehicle charging scheduling.

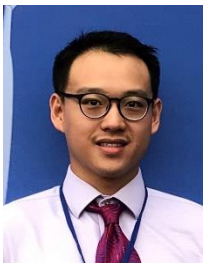

Chun Sing Lai (S'11, M'19, SM'20) received the B.Eng. (First Class Hons.) in electrical and electronic engineering from Brunel University London, London, UK, in 2013, and the D.Phil. degree in engineering science from the University of Oxford, Oxford, UK, in 2019. He is currently a Lecturer with the Department of Electronic and Electrical Engineering, Brunel University London. From 2018 to 2020, he was an UK Engineering and Physical Sciences Research Council Research Fellow with the School of Civil Engineering, University of Leeds, Leeds, UK.

His current research interests are in power system optimization and data analytics. Dr. Lai was the Publications Co-Chair for both 2020 and 2021 IEEE International Smart Cities Conferences. He is the Vice-Chair of the IEEE Smart Cities Publications Committee and Associate Editor for IET Energy Conversion and Economics. He is the Working Group Chair for IEEE P2814 Standard; Associate Vice President for Systems Science and Engineering of the IEEE Systems, Man, and Cybernetics Society (IEEE/SMCS); Chair of the IEEE SMC Intelligent Power and Energy Systems Technical Committee. He is an IET Member and a Chartered Engineer.

Kang Li (M'05–SM'11) received the B.Sc. degree in Industrial Automation from Xiangtan University, Hunan, China, in 1989, the M.Sc. degree in Control Theory and Applications from Harbin Institute of Technology, Harbin, China, in 1992, and the Ph.D. degree in Control Theory and Applications from Shanghai Jiaotong University, Shanghai, China, in 1995. He also received D.Sc. degree in Engineering from Queen's University Belfast, UK, in 2015. Between 1995 and 2002, he worked at Shanghai Jiaotong University, Delft University of Technology and Queen's University Belfast as a research fellow. Between 2002 and 2018, he was a Lecturer (2002), a Senior Lecturer (2007), a Reader (2009) and a Chair Professor (2011) with the School of Electronics, Electrical Engineering and Computer Science, Queen's University Belfast, Belfast, U.K. He currently holds the Chair of Smart Energy Systems at the University of Leeds, UK. His research interests cover nonlinear system modelling, identification, and control, and machine learning, with substantial applications to energy and power systems, smart grid, transport decarbonization, and energy management in energy intensive manufacturing processes. He has authored/co-authored over 200 journal publications and edited/co-edited 18 conference proceedings, winning over 20 prizes and awards, including a recent Springer Nature 'China New Development Award' in 2019 in recognition of the 'exceptional contributions to the delivery of the UN Sustainable Development Goals'.Dr Li was the Chair of the IEEE UKRI Control and Communication Ireland chapter, the Secretary of the IEEE UK & Ireland Section. He is also a visiting professor of Shanghai Jiaotong University, Southeast University, Tianjin University, Shanghai University and Xiangtan University.